Materials Research Letters

ISSN: (Print) 2166-3831 (Online) Journal homepage: http://www.tandfonline.com/loi/tmrl20

Melting of Al Induced by Laser Excitation of 2p Holes

Yudi Rosandi, Fairoja Cheenicode Kabeer, Yaroslav Cherednikov, Eeuwe S. Zijlstra, Martin E. Garcia, Nail A. Inogamov & Herbert M. Urbassek

To cite this article: Yudi Rosandi, Fairoja Cheenicode Kabeer, Yaroslav Cherednikov, Eeuwe S. Zijlstra, Martin E. Garcia, Nail A. Inogamov & Herbert M. Urbassek (2015) Melting of Al Induced by Laser Excitation of 2p Holes, Materials Research Letters, 3:3, 149-155, DOI: 10.1080/21663831.2015.1033564

To link to this article: http://dx.doi.org/10.1080/21663831.2015.1033564

MATERIALS RESEARCH LETTERS

Mater. Res. Lett., 2015
Vol. 3, No. 3, 149–155, http://dx.doi.org/10.1080/21663831.2015.1033564

Taylor & Francis
Taylor & Francis Group

www.tandfonline.com/toc/tmrl20/current

Melting of Al Induced by Laser Excitation of 2p Holes

Yudi Rosandi[a,b], Fairoja Cheenicode Kabeer[c,d], Yaroslav Cherednikov[b], Eeuwe S. Zijlstra[c], Martin E. Garcia[c], Nail A. Inogamov[e] and Herbert M. Urbassek[b]*

[a]*Department of Physics, Universitas Padjadjaran, Jatinangor, Sumedang 45363, Indonesia;* [b]*Fachbereich Physik und Forschungszentrum OPTIMAS, Universität Kaiserslautern, Erwin-Schrödinger-Straße, D-67663 Kaiserslautern, Germany;* [c]*Theoretische Physik, Universität Kassel and Center for Interdisciplinary Nanostructure Science and Technology (CINSaT), Heinrich-Plett-Straße 40, 34132 Kassel, Germany;* [d]*Fritz-Haber-Institut der Max-Planck-Gesellschaft, Faradayweg 4–6, D-14195 Berlin, Germany;* [e]*Landau Institute for Theoretical Physics, Russian Academy of Science, Prospekt Akademika Semenova 1-A, 142432 Chernogolovka, Moscow, Russia*

(*Received 16 February 2015; final form 20 March 2015*)

Novel photon sources—such as XUV- or X-ray lasers—allow to selectively excite core excitations in materials. We study the response of a simple metal, Al, to the excitation of 2p holes using molecular dynamics simulations. During the lifetime of the holes, the interatomic interactions in the slab are changed; we calculate these using WIEN2k. We find that the melting dynamics after core-hole excitation is dominated by classical electron–phonon dynamics. The effects of the changed potential surface for excited Al atoms occur on the time scale of 100 fs, corresponding to the Debye time of the lattice.

Keywords: Laser Materials Processing, XUV Irradiation, Molecular Dynamics, Al

Ultrafast laser-induced melting of metals has been studied theoretically in the past by computer simulation and many aspects are by now well understood.[1–6] Such studies consider the action of a visible-light (VIS) or ultraviolet (UV) laser, which conveys the photon energy to the conduction electrons of the metal. Electron–phonon coupling then equilibrates the energy with the lattice, which is heated and melts. Aspects such as the superheating of the lattice, the nucleation of the liquid phase, or the influence of pre-existing lattice defects, for example, grain boundaries, have been studied.

Apart from this 'conventional' energy transfer via the conduction electron gas, another route of heating the lattice was detected in several materials; the accompanying melting process was termed *non-thermal melting*, as lattice disordering and melting occur so quickly—on the timescale of several 100 fs—that the lattice is not in (local) thermodynamic equilibrium. The process operates via the changed interactions that lattice atoms experience as a consequence of the laser-excited electrons. It has first been found in covalently bonded materials crystallizing in the diamond structure such as C or Si [7–10] and, more recently, also in a wider class of semiconducting and semimetallic materials, for example, in InP [11] and Bi.[12] On the microscopic scale, non-thermal melting can be distinguished from conventional melting by fractionally diffusive atomic pathways.[13]

In the present paper, we inquire how laser-induced changes of the interatomic interaction potential of a simple metal, Al, influence the melting process. VIS or UV lasers will not be able to induce such changes.[14] However, extreme ultraviolet (XUV) pulses with an energy of 75 eV are able to selectively excite 2p core holes in Al atoms. We study their effect on the subsequent lattice dynamics.

We assume the laser pulse to have a Gaussian time distribution with maximum at time $t_0 = 0$ and width σ,

$$S(t) = \frac{E_0}{\sqrt{2\pi}\sigma} \exp\left[-\frac{1}{2}\left(\frac{t-t_0}{\sigma}\right)^2\right]. \qquad (1)$$

Here E_0 is the total energy absorbed by the electrons per unit volume. Due to the large penetration depth of 75 eV

*Corresponding author. Email: urbassek@rhrk.uni-kl.de

photons of around 50 nm,[15] we assume the excitation to occur homogeneously in our Al slab. We choose here $E_0 = 0.0214$, 0.0428, and 0.0856 eV/Å^3; since the atomic volume of Al is $\Omega = 16.39$ Å^3, the lowest energy is equivalent to an energy density of $\epsilon = 0.35$ eV/atom. This is around the melting threshold of Al.[16,17] XUV laser pulse widths of $\sigma = 4$, 40, and 400 fs will be considered.

The laser is assumed to excite Al atoms from their ground state to an excited state Al^{2p}, where a hole in the 2p level has been created. Since the excitation energy is 73.1 eV,[18] the concentration of excited atoms corresponding to the energy density E_0 amounts to $p = 0.45\%$.

The lifetime of the 2p hole equals roughly 40 fs.[19,20] De-excitation occurs mainly via Auger decays, since radiative processes are too slow.[19] We assume that the excitation energy of the 2p hole, 73.1 eV, is put into the conduction band after de-excitation.

As indicated earlier, in our simulations, excited Al atoms, Al^{2p}, are diluted in the specimen. It is therefore reasonable to assume that they only interact with ground-state Al atoms, Al^0. The interaction is calculated using the all-electron full-potential linearized augmented plane-wave code WIEN2k [21][1]: inside a supercell with side lengths $2a \times 2a \times 2a$, where a is the lattice parameter of Al, we create a core hole by removing a $2p_{3/2}$ electron from one Al atom. This electron is added to the conduction band in order to maintain charge neutrality.[22,23] In Figure 1, which shows part of our supercell, the thus excited atom has been colored red. One of the nearest neighbors is then displaced along the line connecting it with the excited atom, as indicated by a purple arrow. The total energy is compared to the total energy of the same supercell with no core hole as a function of the interatomic distance between the two aforementioned atoms. Following our discussion about the nature of many-body interactions in Al below, we assume that the dilute excitation of core holes in Al mostly affects the pair interaction between the excited atom and its nearest neighbors. Neglecting other effects, our computed energy equals the change in the pair potential $\Delta V(r)$ between an excited and a ground-state atom. Our result is plotted in Figure 1. We see that it gives an attractive contribution to the interatomic forces; that is, excited atoms attempt to create lattices with smaller lattice constant. Beyond 3 Å it decreases slightly by 0.02 eV. We believe that this small decrease is due to a slightly incomplete screening within our 32-atom supercell. As shown in Figure 1, we have not included this change in ΔV for $r > 3.0$ Å in our fit.

Figure 2 demonstrates schematically how the excitation of a core hole leads to lattice heating. The potential curves are provided for the so-called effective potentials (see Equation (5)). An initially cold atom moves from the ground-state potential to the excited-state potential

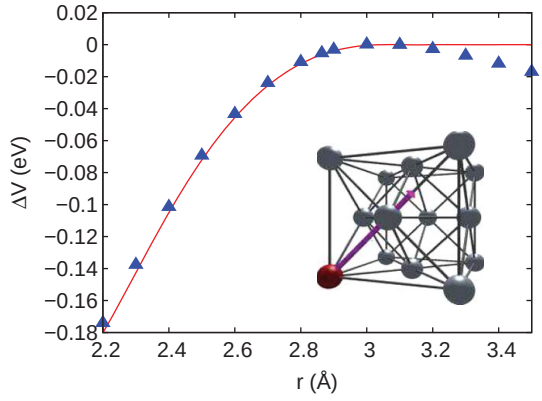

Figure 1. Difference $\Delta V(r)$ between the interaction of an excited atom and a ground-state atom to that between two ground-state atoms. Data points show our results obtained with WIEN2k and the solid line shows the fit to the WIEN2k data that has been used in our molecular dynamics simulations. The inset shows part of the 32-atom supercell used to determine the interaction between a core-hole-excited and a ground-state Al atom: one $2p_{3/2}$ electron has been excited from the red atom to the conduction band. In addition, one of its nearest neighbors is displaced along the line connecting it with the excited atom, as indicated by the purple arrow.

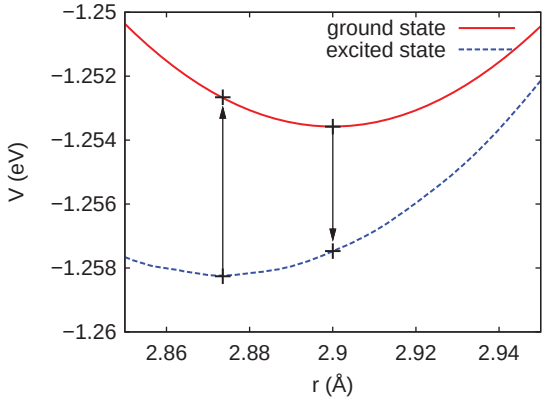

Figure 2. Sketch of the excitation and de-excitation process. The potentials plotted are the effective potentials, Equation (5), for Al^0-Al^0 (ground state) and Al^0-Al^{2p} (excited state). Both transitions are idealized to occur at the respective potential minima; in our simulations, the de-excitation process will occur from a position that may vary for each individual event, due both to thermal motion and to the individual excitation lifetime.

and now feels an attractive force. While moving toward its new equilibrium position, it acquires kinetic energy which will ultimately lead to thermal heating of the lattice. After the lifetime of the excitation, the potential changes back to the ground-state curve; for simplicity, in the figure we assume this to happen at the minimum of the excited potential surface. Thereafter, the atom will move back toward its equilibrium position, again acquiring kinetic energy which eventually heats the lattice.

We employ a molecular dynamics (MD) scheme coupled to the two-temperature model (TTM) to describe

the time evolution of the Al thin film; the coupled code is available.[24] We choose an Al crystal with a (100) surface as the target material. The simulation crystallite consists of 131,072 atoms, arranged in 64 monolayers ($d = 13$ nm). The lateral size amounts to 164 nm^2, arranged in 64×64 monolayers. We employ lateral periodic boundary conditions on the sides of the crystal, while the top and bottom surfaces are left free. A many-body interaction potential of the embedded-atom-model (EAM) type is employed for Al [25] with cutoff radius $R_c = 5.558$ Å. This state-of-the-art potential reproduces the melting properties of Al, such as the melting temperature and the latent heat of melting within 3%.[25]

In EAM potentials, the energy of an atom i is composed of the pair interaction $V(r_{ij})$ depending on the distance r_{ij} of atom i and its neighbors j and a many-body term $F(\rho_i)$,[26,27]

$$E_i = \frac{1}{2}\sum_j V(r_{ij}) + F(\rho_i). \tag{2}$$

Here the electron density at site i, ρ_i, enters as the sum of contributions of all neighboring atoms, $\rho_i = \sum_j g(r_{ij})$. In our system, this expression describes the interaction between ground-state atoms Al^0; the functions V, F, and g are provided in [25]. In our approach, the mixture of Al^{2p} and Al^0 atoms is described by keeping the many-body terms F and g unchanged; however, the pair potential is modified to $V(r_{ij}) + \Delta V(r_{ij})$ in the interaction of an Al^{2p} atom i and an Al^0 atom j (or vice versa).

For small changes in the system, the many-body EAM potential may be approximated by an *effective* pair potential, $V_{\text{eff}}(r)$.[26,28] This can be shown as follows. The energy E_i, Equation (2), does not change under the transformation

$$\tilde{F}(\rho) = F(\rho) - c\rho, \quad \tilde{V}(r) = V(r) + 2cg(r), \tag{3}$$

with constant c. Now let ρ_0 denote the value of the electron density at a ground-state Al^0 atom in the equilibrium lattice and choose $c = F'(\rho_0)$. Then, a Taylor expansion of $F(\rho)$ around ρ_0 shows that

$$\tilde{F}(\rho) = \tilde{F}(\rho_0) + \tfrac{1}{2}(\rho - \rho_0)^2 F''(\rho_0) + \cdots \tag{4}$$

up to terms of third or higher order in $\rho - \rho_0$. Thus, small changes in the electron density ρ around the equilibrium value will not influence E_i nor the atom dynamics in this representation. The pertinent pair potential $\tilde{V}(r)$ gives then the *effective* pair potential

$$\tilde{V}(r) = V_{\text{eff}}(r) = V(r) + 2F'(\rho_0)g(r). \tag{5}$$

This argument shows that for small changes in the EAM system, the dynamics can be described by an effective pair potential; this fact justifies our assumption that dilute excitations in Al can be described by a change in the pair potential. The corresponding effective potential for a dilute Al^{2p} surrounded by Al^0 is then $V_{\text{eff}}(r) + \Delta V(r)$; both effective potentials are plotted in Figure 2.

The excitation of Al atoms is treated as a random process: we excite Al atoms in the slab with a time-dependent probability distribution proportional to the laser profile (Equation (1)). While excited, the interaction of Al^{2p} atoms to ground state Al^0 atoms is governed by a different interaction (Figure 1). De-excitation occurs randomly with an exponentially distributed individual lifetime around a mean lifetime of 40 fs. Then, the interaction switches back to the ordinary Al^0-Al^0 interaction, while the energy of 73.1 eV is given to the electronic system.

The TTM, which has been introduced more than 30 years ago for describing electron emission from metals,[29] is commonly used to characterize the energy transfer between the electronic system and the lattice. In this model, the electron and atomic temperatures are connected by a coupling factor that controls the electron–phonon relaxation time. In our case, where an ultrathin Al film is considered, the electron temperature swiftly homogenizes due to the fast electron diffusion. The electron temperature T_e is calculated from

$$C_e(T_e)\frac{dT_e}{dt} = -G(T_e)[T_e - T_a] + \tilde{S}(t), \tag{6}$$

where C_e denotes the electronic heat capacity and G the coupling factor. $\tilde{S}(t)$ is the source term. In contrast to VIS or UV laser excitations, where the source simply equals the laser profile, Equation (1), in our case, $\tilde{S}(t)$ equals a sum of Dirac delta functions, $(73.1\text{ eV}) \cdot \delta(t - t')$, with t' the times when Al^{2p} core holes decay. The electronic heat capacity and the coupling depend on the electron temperature as described in [30]. T_a denotes the average atom temperature in the sample.

Atom dynamics is calculated by MD. We characterize the state of the system using the local temperature $T_{a,i}$ of atom i. It is determined as an average over all N_i atoms in a sphere (volume V_c) of radius R_c, equal to the cutoff radius of the potential, around atom i [5,31]:

$$\frac{3}{2}N_i k T_{a,i} = \sum_{j=1}^{N_i}\frac{m}{2}(\mathbf{v}_j - \boldsymbol{V}_i)^2, \tag{7}$$

where m is the atom mass, k is the Boltzmann constant, j enumerates the atoms in V_c, $\mathbf{v}_j$ is their velocity, and $\boldsymbol{V}_i$ is the average velocity of all atoms within this sphere.

Electronic energy is given to the atoms by scaling the thermal velocities of the atoms at every MD time step. That is, energy is given only as *thermal energy* to the atoms. The energy input to atom i, ΔE_i, is calculated from the temperature difference of the atomic and

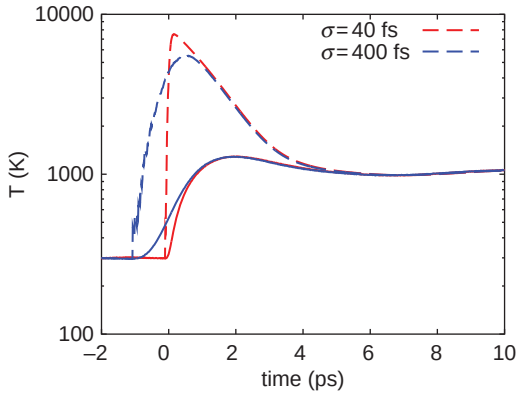

Figure 3. Temporal evolution of the electron (dashed line) and atom (solid line) temperatures in the XUV laser-excited slab ($p = 0.45\%$) for two values of the pulse width σ.

electronic system at the corresponding time step Δt,

$$\Delta E_i = G(T_e)[T_e - T_{a,i}]\Delta t. \quad (8)$$

The simulations are started with a system equilibrated at 300 K at a time of $t = -5$ (-7) ps for $\sigma = 40$ (400) fs. At this time, the TTM solver is inserted after every MD computation step and solves Equation (6), providing the change of electron temperatures for the next MD time step. Details are provided in [17]. The atom trajectories are followed up to time $t = 20$ ps.

In Figure 3, we compare how the electronic and atomic temperatures evolve as a function of time after irradiation. The high initial electron temperature of 7744 K decreases within around 5 ps to its equilibrium value of 1042 K. Simultaneously the atom temperature T_a increases and reaches a maximum after around 2 ps. Thereafter, temperature slightly decreases due to the global adiabatic film expansion and the latent heat of the melting process.

Since the long-time thermodynamics in the films is identical for the two pulses studied (Figure 3), we show as an example atomistic snapshots of the dynamics in the melting film for the $\sigma = 400$ fs laser pulse (Figure 4).

The atoms have been colored according to the local-order parameter, which describes whether the structure is crystalline or molten. It is calculated according to [1,2,32]. In short, we define the local-order parameter η_i of atom i as

$$\eta_i = \left| \frac{1}{Z} \sum_{j=1}^{Z} \frac{1}{6} \sum_{k=i}^{6} \exp(i\boldsymbol{q}_k \cdot \boldsymbol{r}_{ij}) \right|^2, \quad (9)$$

where Z is the number of first- and second-nearest neighbors. The six wave vectors $\boldsymbol{q}_k$ are characteristic of the fcc structure and are chosen such that $\exp(i\boldsymbol{q}_k \cdot \boldsymbol{r}_{ij}) = 1$ for all vectors $\boldsymbol{r}_{ij}$ connecting an atom i to its first- or second-nearest neighbors j in the perfect fcc lattice. The (global)-order parameter η is then the average over the local-order parameters of all atoms in the system.

Values larger than a threshold value—here taken as 0.05—indicate a crystal, and smaller values a liquid. It is seen that at 2 ps the aluminum film still has maintained a high degree of crystallinity. Melting then starts from the surface and moves inward. Since the excitation was chosen such that the film is just about to melt, we see that even at 5 ps a small part of the film still has retained some order in the center of the film. We note that the fact that melting starts from the surface (as inhomogeneous melting) is in agreement with previous studies of ultrafast laser-induced melting.[3,17]

We explore the effect of a higher excitation density in Figure 5. In addition to the case of a concentration of core holes of $p = 0.45\%$ considered up to now, we now also use values of $p = 0.90$ and 1.80%. Correspondingly also the energy density increases from $\epsilon = 0.35$ to 0.70 and 1.40 eV/atom, moving far above the melting threshold. A laser pulse width of only 4 fs was used in order to separate the excitation and de-excitation of the core holes clearly in time from the lattice dynamics. We see that due to higher excitation density melting occurs faster—the melting time decreases from 4 over 2 to 1 ps. This effect has been observed previously in simulations of ultrashort-pulse melting of Cu thin films.[5]

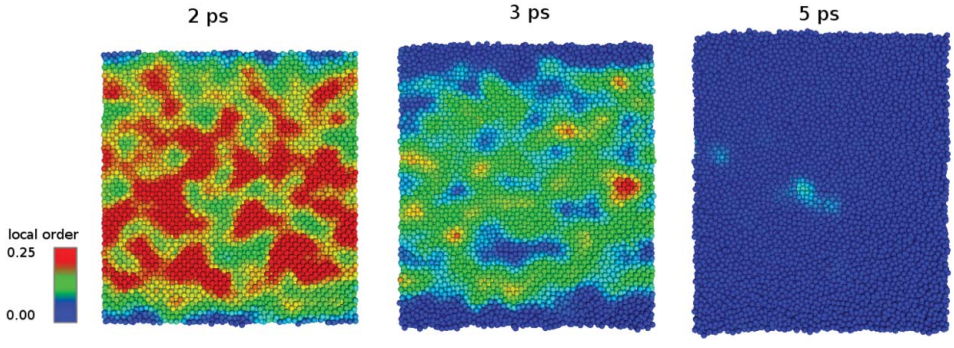

Figure 4. Snapshots of the Al film at times of 2, 3 and 5 ps after XUV laser irradiation with a pulse length of 400 fs. Color denotes the local-order parameter.

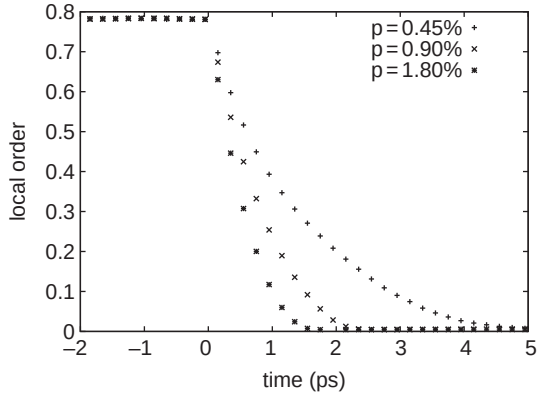

Figure 5. Time evolution of the local-order parameter in the XUV-laser-irradiated slab for various concentrations p of core holes and a laser pulse width $\sigma = 4$ fs.

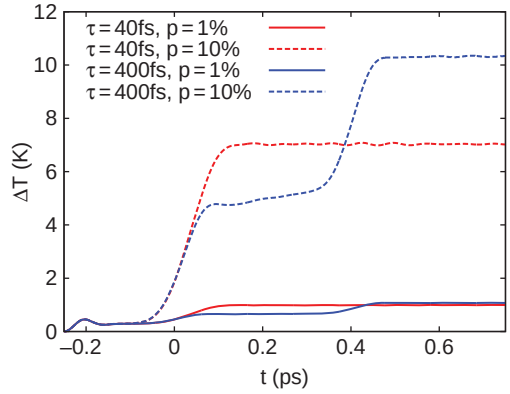

Figure 6. Change in lattice temperature caused by core-hole excitation and de-excitation of Al atoms. Results are shown for the actual lifetime of the core hole of $\tau = 40$ fs and also for an artificially increased lifetime of $\tau = 400$ fs. Results are provided for two values of the concentration p of core holes in the lattice for an XUV laser pulse of 40 fs width.

In order to understand in more detail the action of the lattice heating by core holes, we first discuss with the help of Figure 2 the size of the energy transfer to the lattice that is to be expected due to the sudden potential changes; note that the numbers provided are valid for the effective potentials described earlier (Equation (5)). Initially atoms are on the ground-state potential and have equilibrium distances of 2.90 Å. After the sudden excitation they move toward the new equilibrium value of 2.87 Å, delivering a maximum of 0.7 meV to thermal energy. Let us assume that the atoms are de-excited when they are in their new equilibrium location; after returning to the ground-state potential surface they deliver 0.92 meV. The total energy transfer to the lattice amounts to 1.62 meV per bond; this adds up to 19.4 meV when taking into account that each Al^{2p} atom has 12 Al^{0} nearest neighbors. The actual situation is more complex, since the exact position from which atoms are de-excited is not fixed, due both to thermal motion and to the individual excitation lifetime; so the above numbers are upper estimates.

In order to quantitatively assess the lattice heating by core holes, we performed a model simulation in which we suppress artificially the heating of the electron gas by setting the electron–phonon coupling $G = 0$ in Equation (6). Thus, the only action of the excitation of the core electrons is via the changed interatomic potential ΔV (Figure 1). Figure 6 shows the temperature gain in the lattice due to the excitation and de-excitation processes. In order to emphasize the effect, we increased the concentration of excited atoms in the target up to 10%; in addition, we used deterministic lifetimes in order to clearly separate the effects of excitation and de-excitation. The small temperature increase before the start of the laser pulse is due to incomplete target relaxation.

Results are displayed for the actual lifetime of 2p holes of $\tau = 40$ fs. For demonstration purposes, the simulation was also performed for an artificially increased lifetime of $\tau = 400$ fs—larger than the Debye time of the solid. This separates the excitation process (during the laser pulse, at 0 ps) and the de-excitation process (at 0.4 ps). The figure shows that both processes add to target heating due to the potential switching. For the natural lifetime, the effects of excitation and de-excitation overlap; the combined effect is smaller than for the 400 fs demonstration case, since atoms are already de-excited while they are still in the vicinity of their original position and have not gained much kinetic energy. The time scale of the effect is 100 fs—around the Debye time. We conclude that for a concentration of $p = 10\%$ of excited atoms, the energy transfer to the lattice corresponds to 10 K, or equivalently to roughly 1 meV per atom in the lattice. This means each Al^{2p} contributed about 10 meV during excitation and de-excitation to lattice heating, in good agreement with the discussion above.

We study the melting of Al induced by a short-pulse excitation of 2p core-hole states. Our model includes both the heating of the lattice by conduction electrons (electron–phonon coupling) and the heating induced by the changed potential energy surfaces of ground-state and excited Al atoms.

We find that for the specific case of Al the melting dynamics is dominated by classical electron–phonon dynamics. The effects of the changed potential surface for XUV-excited Al atoms are minor. We note that this study is to the best of our knowledge the first of its kind and that the influence of dilute excitation of core holes in other materials is unknown.

The lattice heating induced by the changed potential surface for excited Al atoms occurs on the time scale of 100 fs, corresponding to the Debye time of the lattice. We expect that the effect can be amplified by using temporally structured laser pulses, such as double-peak

laser pulses, which repeatedly induce potential surface changes of the Al atoms.

Acknowledgments We acknowledge discussions with H.C. Schneider and S. Kaltenborn. YR is grateful for funding from the Indonesian Directorate General of Higher Education (DIKTI), contract no. 393/UN6.R/PL/2015, and appreciates the computational resources provided by the computer cluster 'Elwetritsch' of the University of Kaiserslautern. ESZ and MEG thank the Deutsche Forschungsgemeinschaft for financial support through the project GA 465/16-1/ZI 1307/1-1 and the ITS in Kassel for computing power. NI thanks support from the Russian Science Foundation grant 14-19-01599.

Disclosure statement No potential conflict of interest was reported by the authors.

Note

1. In our calculations, the muffin-tin spheres centered around the Al atoms have a radius of $r_{MT} = 1.09$ Å. Linearized augmented plane waves with $r_{MT}K < 6.0$, where $K = |\mathbf{K}|$ is the absolute value of the **K**-vector of the plane wave, have been included in the basis set. The Brillouin zone of the 32-atom supercell has been sampled by a $10 \times 10 \times 10$ **k**-grid. We have used the local density approximation.

ORCID

Herbert M. Urbassek http://orcid.org/0000-0002-7739-4453

References

[1] Ivanov DS, Zhigilei LV. Combined atomistic-continuum modeling of short-pulse laser melting and disintegration of metal films. Phys Rev B. 2003;68:064114.
[2] Upadhyay AK, Urbassek HM. Melting and fragmentation of ultra-thin metal films due to ultrafast laser irradiation: a molecular-dynamics study. J Phys D: Appl Phys. 2005;38:2933–2941.
[3] Lin Z, Zhigilei LV. Time-resolved diffraction profiles and atomic dynamics in short-pulse laser-induced structural transformations: molecular dynamics study. Phys Rev B. 2006;73:184113.
[4] Ivanov DS, Zhigilei LV. Kinetic limit of heterogeneous melting in metals. Phys Rev Lett. 2007;98:195701.
[5] Upadhyay AK, Urbassek HM. Effect of laser pulse width on material phenomena in ultrathin metal films irradiated by an ultrafast laser: molecular-dynamics study. J Phys D: Appl Phys. 2007;40:3518–3526.
[6] Lin Z, Leveugle E, Bringa EM, Zhigilei LV. Molecular dynamics simulation of laser melting of nanocrystalline Au. J Phys Chem C. 2010;114:5686–5699.
[7] Shank CV, Yen R, Hirlimann C. Time-resolved reflectivity measurements of femtosecond-optical-pulse-induced phase transitions in silicon. Phys Rev Lett. 1983;50:454–457.
[8] Stampfli P, Bennemann KH. Theory for the instability of the diamond structure of Si, Ge, and C induced by a dense electron-hole plasma. Phys Rev B. 1990;42:7163–7173.
[9] Stampfli P, Bennemann KH. Time dependence of the laser-induced femtosecond lattice instability of Si and GaAs: role of longitudinal optical distortions. Phys Rev B. 1994;49:7299–7305.
[10] Zier T, Zijlstra ES, Garcia ME. Silicon before the bonds break. Appl Phys A. 2014;117:1–5.
[11] Bonse J, Wiggins SM, Solis J. Dynamics of femtosecond laser-induced melting and amorphization of indium phosphide. J Appl Phys. 2004;96:2352–2358.
[12] Sciaini G, Harb M, Kruglik SG, Payer T, Hebeisen CT, Meyer zu Heringdorf F-J, Yamaguchi M, Horn-von Hoegen M, Ernstorfer R, Miller RJD. Electronic acceleration of atomic motions and disordering in bismuth. Nature. 2009;458:56–59.
[13] Zijlstra ES, Kalitsov A, Zier T, Garcia ME. Fractional diffusion in silicon. Adv Mater. 2013;25:5605–5608.
[14] Recoules V, Clérouin J, G Zérah , Anglade PM, Mazevet S. Effect of intense laser irradiation on the lattice stability of semiconductors and metals. Phys Rev Lett. 2006;96:055503.
[15] Carron NJ. An introduction to the passage of energetic particles through matter. New York: Taylor and Francis Group; 2007.
[16] Rosandi Y, Urbassek HM. Ultrashort-pulse laser irradiation of metal films: the effect of a double-peak laser pulse. Appl Phys A. 2010;101:509–515.
[17] Rosandi Y, Urbassek HM. Melting of Al by ultrafast laser pulses: dynamics at the melting threshold. Appl Phys A. 2013;110:649–654.
[18] Bearden JA, Burr AF. Reevaluation of X-ray atomic energy levels. Rev Mod Phys. 1967;39:125–142.
[19] Keski-Rahkonen O, Krause MO. Total and partial atomic-level widths. At Data Nucl Data Tables. 1974;14:139–146.
[20] Almbladh C-O, Morales AL, Grossmann G. Theory of Auger core-valence-valence processes in simple metals. I. Total yields and core-level lifetime widths. Phys Rev B. 1989;39:3489–3502.
[21] Blaha P, Schwarz K, Madsen GKH, Kvasnicka D, Luitz J. WIEN2k, an augmented plane wave plus local orbitals program for calculating crystal properties. Austria: Vienna University of Technology; 2001.
[22] Zijlstra ES, Cheenicode Kabeer F, Bauerhenne B, Zier T, Grigoryan N, Garcia ME. Modeling of material properties after ultrashort laser and XUV excitation. Appl Phys A. 2013;110:519–528.
[23] Kabeer FC, Zijlstra ES, Garcia ME. Road of warm dense noble metals to the plasma state: *Ab initio* theory of the ultrafast structural dynamics in warm dense matter. Phys Rev B. 2014;89:100301(R).
[24] The MD code. Available from: http://merapiphysikuni-klde/objectmd/
[25] Ercolessi F, Adams JB. Interatomic potentials from first-principles calculations: the force-matching method. Europhys Lett. 1994;26:583–588.
[26] Carlsson AE. Beyond pair potentials in elemental transition metals and semiconductors. In: Ehrenreich H, Turnbull T, editors. Solid state physics. Vol. 43. Boston (MA): Academic Press; 1990. p. 1.
[27] Daw MS, Foiles SM, Baskes MI. The embedded-atom method: a review of theory and applications. Mater Sci Rep. 1993;9:251–310.
[28] Foiles SM. Application of the embedded-atom method to liquid transition metals. Phys Rev B. 1985;32:3409–3415.
[29] Anisimov SI, Kapeliovich BL, Perel'man TL. Electron emission from metal surfaces exposed to ultrashort laser pulses. Sov Phys JETP. 1974;39:375–377.
[30] Lin Z, Zhigilei LV, Celli V. Electron-phonon coupling and electron heat capacity of metals under conditions of strong electron-phonon nonequilibrium. Phys Rev B. 2008;77:075133. Available from: http://wwwfaculty virginiaedu/CompMat/electron-phonon-coupling/

[31] Colla ThJ, Urbassek HM. Visualization of keV-ion-induced spikes in metals. Radiat Eff Defects Solids. 1997;142:439–447.

[32] Morris JR, Song X. The melting lines of model systems calculated from coexistence simulations. J Chem Phys. 2002;116:9352–9358.